

# Series-Fed Omnidirectional mm-Wave Dipole Array

Neeraj Kumar Maurya<sup>1b</sup>, *Graduate Student Member, IEEE*, Max J. Ammann<sup>1b</sup>, *Fellow, IEEE*,  
and Patrick McEvoy, *Senior Member, IEEE*

**Abstract**—A compact series-fed, omnidirectional printed dipole array for millimeter-wave (mm-wave) bands n257, n259, and n261 is proposed. A series feed technique with microstrip to grounded-co-planar waveguide (CPW) transition was used to feed the antenna. The prototype was fabricated and measured for the range from 27.25 to 28.5 GHz. The measured peak gain is 10.3 dBi with a maximum azimuthal ripple of 4.4 dB.

**Index Terms**—Azimuthal gain ripple, leaky wave antennas (LWAs), millimeter-wave (mm-wave) omnidirectional, series fed.

## I. INTRODUCTION

THE rapid expansion in the millimeter-wave (mm-wave) frequency domain has completely changed the course of wireless communication. One of the most important steps to make smart cities, the Internet-of-Things (IoT), smart homes, and vehicular communication a reality is to use mm-wave frequencies for wireless applications. The rise in the number of wireless appliances has also led to a rise in data traffic [1]. The adoption of mm-wave frequencies enabled several gigahertz of bandwidth, allowing data rate and latency limits to be exceeded. The availability of a broad electromagnetic spectrum and frequency reusability are the most important characteristics of mm-wave deployment [2].

Although mm-wave systems have a shorter effective communication distance than microwave systems due to increased propagation loss, they are sufficient to cover small cells that span hundreds of meters [3]. So, the use of mm-wave systems in providing high-speed wireless connectivity in indoor venues, such as shopping centers, stadiums, and auditoriums, is very effective. To satisfy the network coverage in such scenarios, omnidirectional antennas for mm-wave frequencies are key. High gain antennas are also required to mitigate losses due to obstacles, including walls, buildings, and trees, which makes the mm-wave bands more beneficial as larger antenna arrays can be realized in small form factor.

Many omnidirectional designs were proposed for the sub-6 GHz band [4], [5], [6], [7]. The collinear array design in [4] used back-to-back microstrip patches providing an omnidirectional pattern at 2.586 GHz. This design has narrow bandwidth

due to the inherent nature of the microstrip elements. As the feed point is on the patch, it confines this for use as an integrated design and cannot be scaled to mm-wave as the feed width dimension is comparable to the patch width for the given impedance.

In [5], an omnidirectional antenna array was proposed using back-to-back microstrip elements and a modified feed point placed on the antenna edge. Back-to-back elements were also used in a series-fed microstrip antenna operating at 12.5 GHz [6]. Another back-to-back microstrip design with chamfered edges was used to generate circular polarization [7].

In [8] and [14], various mm-wave microstrip and dipole-based designs were presented. Among those, mm-wave omnidirectional antennas are described in [12] and [14]. In [12], an array was designed using a planar solution by placing two dipoles on opposite sides of a substrate-integrated waveguide (SIW) cavity, which was utilized to feed dipoles while maintaining omnidirectional patterns. Then, by using microstrip lines, an omnidirectional array was created by cascading eight cavities. The extension of this work [13] was carried out by creating an omnidirectional antenna design with the inclusion of the corporate-series feed network. A novel series-fed SIW quadrupole antenna [14] was presented for omnidirectional patterns. However, all these designs use surface-integrated waveguides. SIWs use vias in large numbers to develop the design. Insertion of through-plated vias around the resonating structure requires high precision. The via dimensions are also quite critical. In [12] and [14], the azimuthal gain ripple (difference of maximum to minimum gain on azimuth pattern) varies from 7 to 10 dB. Omnidirectional antennas should have a small gain ripple in the azimuth plane. In [15], a hexagonal array consisting of six leaky wave antennas (LWAs) is developed to provide azimuthal omnidirectional coverage. At mm-wave frequencies, where the connector plane is comparable with the antenna dimension, the ground plane transition and feed play an important role in omnidirectionality.

In this article, a novel mm-wave series-fed printed dipole array is proposed. In this design, the grounded co-planar waveguide (CPW)–connector interface is introduced for the omnidirectional antenna. This interface makes the design more appropriate for industrial applications. The design has the smallest azimuthal gain ripple of 4.4 dB among the referenced antennas. Furthermore, the peak gain variation across the bandwidth is only 1.5 dB for this antenna. A comparison of the radiation performance with reported antennas is given in Section V.

CST microwave studio suite was used to model the array. The array has a high gain of 9.3 dBi and a broad impedance bandwidth of 1.25 GHz (fractional bandwidth of 4.48%) for

Manuscript received 10 May 2022; revised 9 November 2022; accepted 10 November 2022. Date of publication 4 January 2023; date of current version 3 February 2023. This work was supported by the Science Foundation Ireland under Grant 18/CRT/6222. (*Corresponding author: Neeraj Kumar Maurya.*)

The authors are with the Antenna and High Frequency Research Centre, School of Electrical and Electronic Engineering, Technological University Dublin, Dublin 7, D07 ADY7 Ireland (e-mail: Neerajmaurya34@gmail.com; max.ammann@TUDublin.ie).

Color versions of one or more figures in this article are available at <https://doi.org/10.1109/TAP.2022.3232240>.

Digital Object Identifier 10.1109/TAP.2022.3232240

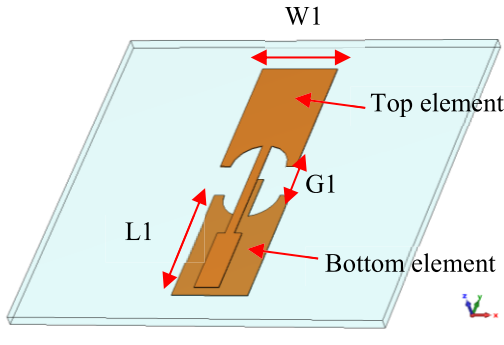
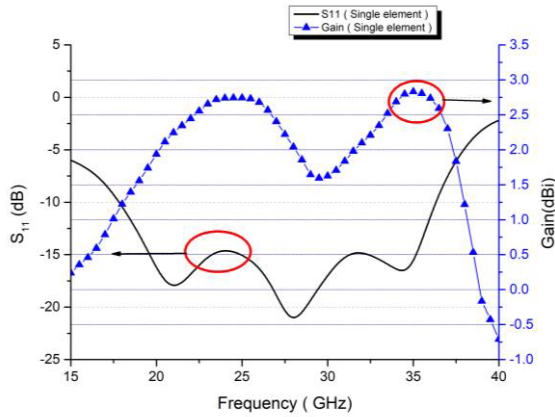


Fig. 1. Printed dipole geometry.


 Fig. 2. Simulated  $S_{11}$  and gain chart for single element.

$S_{11} \leq -15$  dB. The array has a small footprint of only  $67 \times 25$  mm ( $6.23 \lambda_0$ ), as well as a low-cost, low-profile, and easy manufacturability.

## II. PRINTED DIPOLE ANTENNA ELEMENT DESIGN

### A. Broadband Omnidirectional Printed Dipole Design

The dipole elements are printed on opposite sides of the laminate, as shown in Fig. 1. The laminate used is RO5880 with  $\epsilon_r = 2.2$ ,  $\tan\delta = 0.0009$ , substrate thickness of 0.5 mm, and conductor thickness of 0.035 mm.

The dipole elements are separated by  $G1$ . A semicircular cutout is used to increase the dipole bandwidth. This element was designed for a series-fed array, and the extruded part from the bottom element is purposefully optimized to connect the cascaded elements in a series-fed array. The frequency band is 27.25–28.5 GHz. These frequency ranges have been chosen to incorporate the mm-wave bands n257, n261, and n258.

### B. Antenna Design Radiation Characteristics

Fig. 2 shows the  $-10$  dB impedance bandwidth from 17 to 36 GHz. The simulated gain for the single dipole element is shown to vary from 1 to 2.7 dBi from 17 to 36 GHz. The dip in gain at 28.5 GHz is due to a comparatively smaller azimuthal gain ripple.

### C. Impact of the Semicircular Cutout

This curved cutout provides additional design parameters to increase the bandwidth. Additional resonances provided by

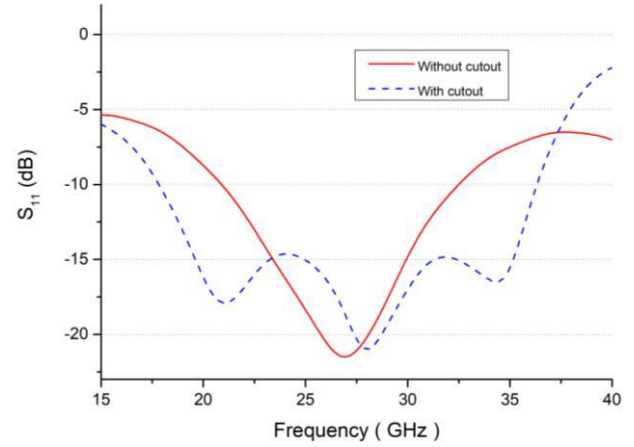
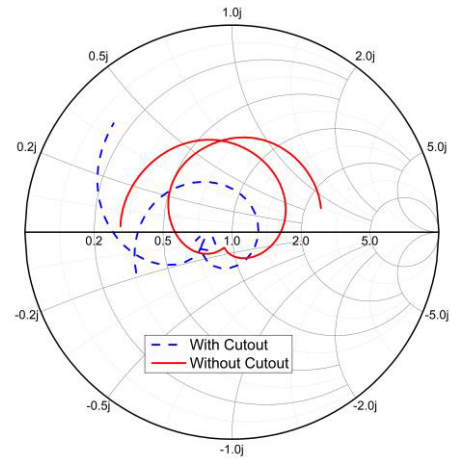

 Fig. 3. Simulated  $S_{11}$  showing the impact of the semicircular cutout.


Fig. 4. Simulated Smith chart showing the impedance variation.

the semicircular structure enhance the bandwidth, as shown in Fig. 3. The fractional bandwidth increased from 42.9% to 72.7% due to the cutout. Fig. 4 shows the antenna input impedance on the Smith chart.

### D. Subarray Design and Feed Method Selection

The series feed was chosen because a corporate feed requires more space than the series-feed array. The total copper trace length would be greater for the corporate feed with more copper losses, which eventually impact the overall gain.

The most important factor for choosing a series-feed technique is that corporate feed networks provide an unavoidable ground plane underneath the feed and in close proximity to the radiating element. This results in a null on the side of the feed network and degrades the omnidirectionality properties.

## III. HIGH-GAIN OMNIDIRECTIONAL PRINTED DIPOLE ARRAY

### A. Series-Fed Array

The six-element series-fed array shown in Fig. 5 was prototyped. The resonator length is slightly less than half of the guided wavelength at 28.25 GHz. For the standard resonator array antenna, each  $\lambda_g/2$  dipole element is separated by a  $\lambda_g/2$

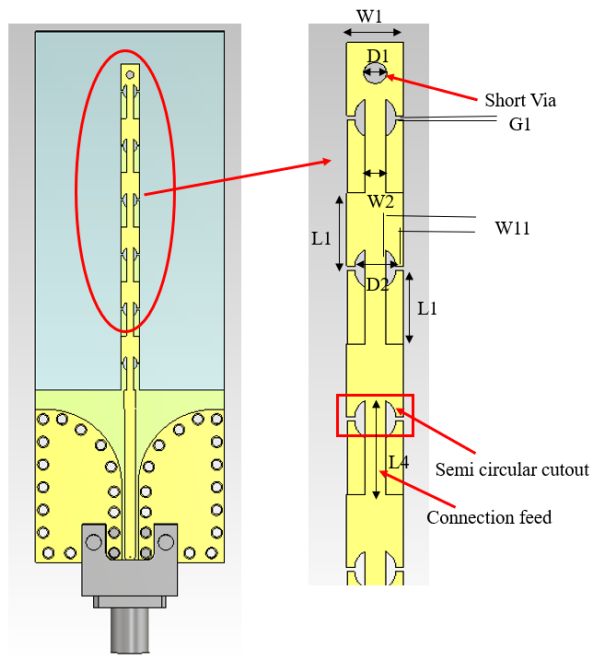


Fig. 5. Antenna array design.

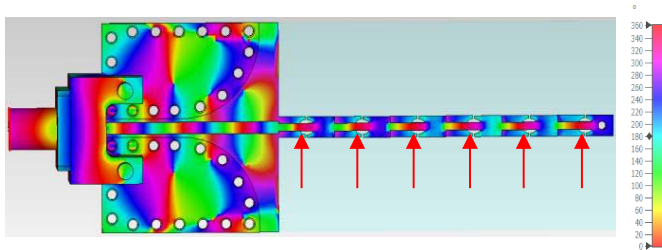


Fig. 6. Phase progression (top view).

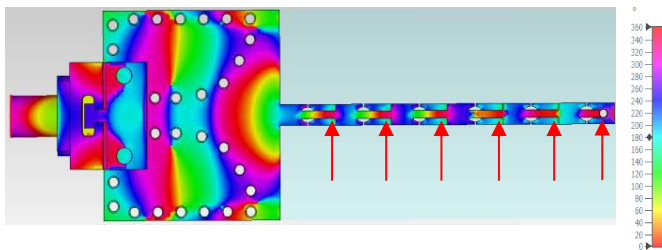


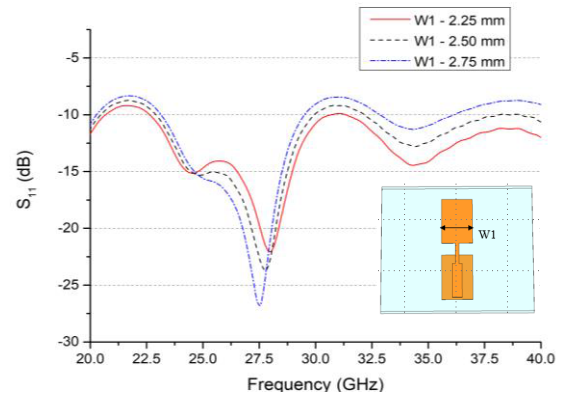
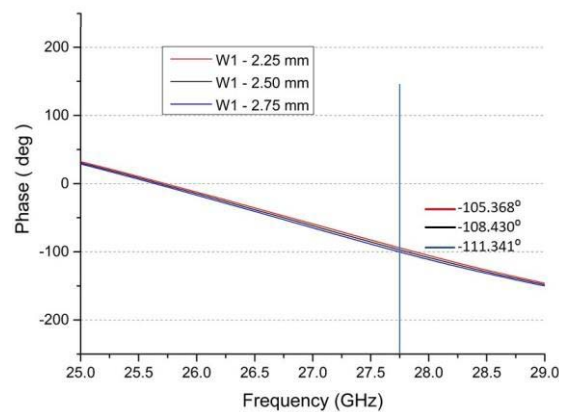
Fig. 7. Phase progression (rear view).

transmission line. When excited, this arrangement will provide the same phase or constant phase difference between antenna elements of the series-fed array.

The connecting via between the top and bottom layer mitigates the issue of floating ground for the surface current and also synchronizes the phase between the dipole elements on opposite sides of the substrate, as shown in Figs. 6 and 7.

### B. Complexities in Series Feed Design for the mm-Waveband

One of the most crucial factors in the series feed is to control the phase across the design, particularly at mm-wave

Fig. 8. Simulated  $S_{11}$  shows dependence on  $W1$ .Fig. 9. Simulated phase shows dependence on  $W1$ .

frequencies. The electrical wavelength at 28.25 GHz on the substrate is 7.85 mm corresponding to a  $45.84^\circ$  per mm change in length.

Second, the small ground plane impacts the radiation patterns and the feed length ( $L4$ ) tunes the radiating element phase.

Third, the proper feed transition allows for use either with connectors or integrated with a radio PCB. The phase dependency on the feed length is also addressed in the design.

### C. Novel Antenna Array Design

For the dipole without the semicircular cutout, the impedance matching is sensitive to the width  $W1$ . As can be seen in Fig. 8, the resonance is also somewhat sensitive to  $W1$ , and it shifts downward with increased width  $W1$  while keeping the length of the dipole element constant. At mm-wave frequencies, the order of these dimensional variations can occur due to manufacturing tolerances. Therefore, it is challenging to maintain equal phase variation across each element in a series-fed array while matching the impedance. The variation of phase with the variation of  $W1$  is shown in Fig. 9.

The novel semicircular cutout structure provides a solution to this issue of phase variation while matching the antenna.

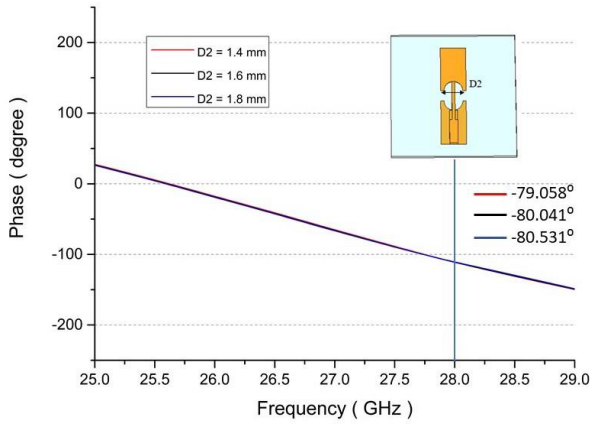


Fig. 10. Simulated phase dependence on cutout diameter  $D_2$ .

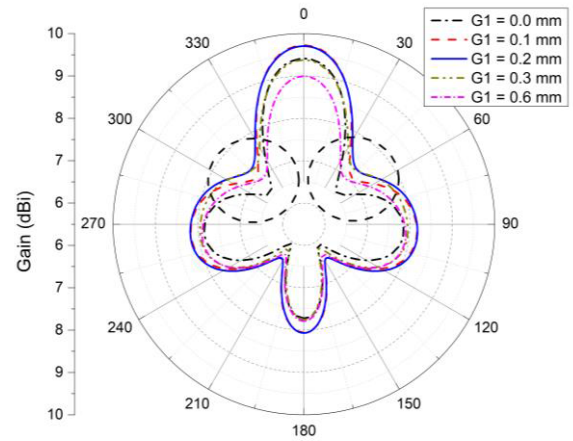


Fig. 12. Simulated azimuthal gain ripple of overlapping and nonoverlapping dipoles.

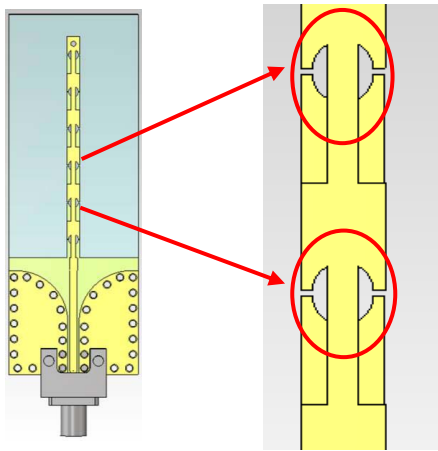


Fig. 11. Antenna design highlighting nonoverlapping dipoles.

Fig. 10 shows that the cutout also tunes the phase between the elements with the precision of  $1^\circ$  resolution. This provides another degree of freedom to tune the phase. The novel structure also provides even power distribution to all elements.

Most reported designs emphasize peak gains for omnidirectional antennas. It is important to have minimum azimuthal gain ripple. In this design, the top and bottom dipole elements are nonoverlapping, as shown in Fig. 11.

Fig. 11 highlights the nonoverlapping dipole elements, and Fig. 12 shows the azimuthal gain ripple. The simulation results show that nonoverlapping dipoles ( $G1 > 0$ ) produce better gain at  $\pm 45^\circ$  and provide smaller azimuthal gain ripple than the overlapping dipoles. The best pattern is achieved at  $G1 = 0.2$  mm. Table I provides the optimized design parameters.

TABLE I  
DESIGN PARAMETERS LIST

Parameter	$W1$	$W11$	$W2$	$D1$	$D2$
Value (mm)	2.5	0.35	0.9	1.1	0.9
Parameter	$G1$	$G2$	$L1$	$L2$	$W3$
Value (mm)	0.2	0.4	3.5	2.5	1.5
Parameter	$W4$	$L3$	$L4$		
Value (mm)	1.3	20.3	4.48		

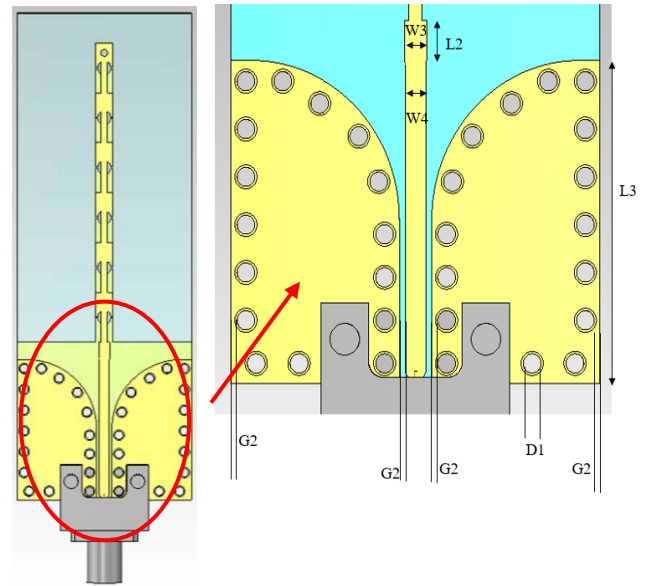


Fig. 13. Antenna feed transition design.

#### IV. NOVEL ANTENNA FEED TRANSITION

The antenna feed transition is one of the most important parts of the design as it determines whether the antenna will work as connectorized or integrated with the RF board.

Fig. 13 shows the antenna transition to the connectors. This design has a microstrip-grounded CPW (MS-GCPW) feed. There is a small microstrip line of length  $L_2$  and width  $W_3$ , which is connected to a grounded CPW, which gives better

impedance bandwidth. It also provides a smooth transition between the antenna and the ground in terms of phase. This section makes the design less sensitive to ground plane dimensions. The tapered edges of grounded CPW provide a smooth transition from microstrip at mm-wave frequencies. The ease of manufacturability is considered while optimizing the dimensions. The connected vias are through plated holes

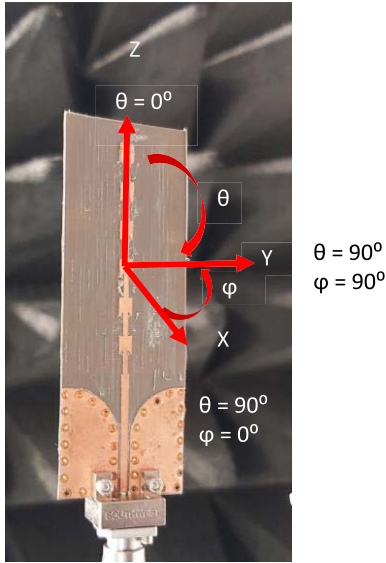
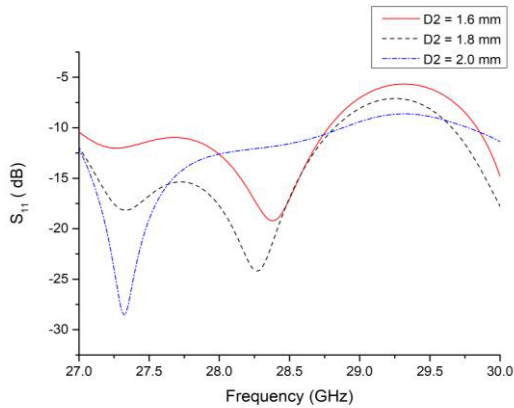


Fig. 14. Measurement coordinate system.

Fig. 15. Simulated  $S_{11}$  for various cut-out diameters.

and are easily manufactured. The 67 mm overall length comprises 44.2 mm for the six radiating elements and 22.8 mm for the feed line. The antenna is designed using a longer feed line to mitigate the feed line phase dependency in the series-fed antenna. This makes the proposed design a more attractive choice for mm-wave integrated antenna designs.

## V. SIMULATED AND MEASURED RESULTS AND ANALYSIS

Fig. 14 shows the coordinate system used for the radiation pattern measurements.

The simulations include the connector in the design. Fig. 15 shows the simulated  $S_{11}$  dependence on the semicircular cut-out diameter.

The  $S_{11}$  result in Fig. 15 shows that the cut diameter impacts the impedance matching. In Fig. 16, it can be seen that a 15 dB return loss provides a total efficiency of 88% at 28.25 GHz.

The measured and simulated  $S_{11}$  are shown in Fig. 17 with reasonable agreement. The measured  $S_{11}$  is  $\leq -15$  dB from 27.25 to 28.5 GHz.

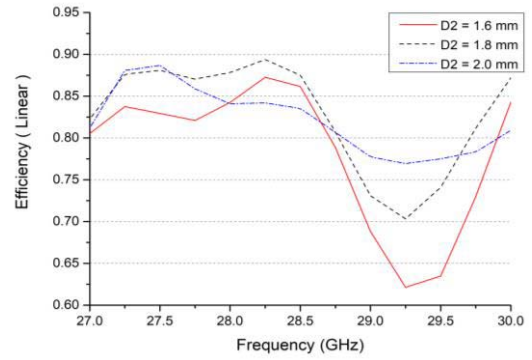


Fig. 16. Simulated efficiency for various cut-out diameters.

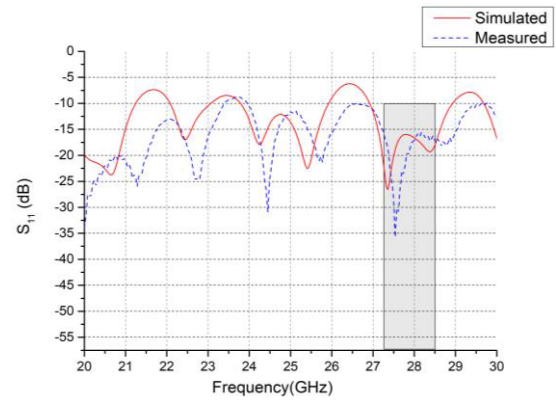
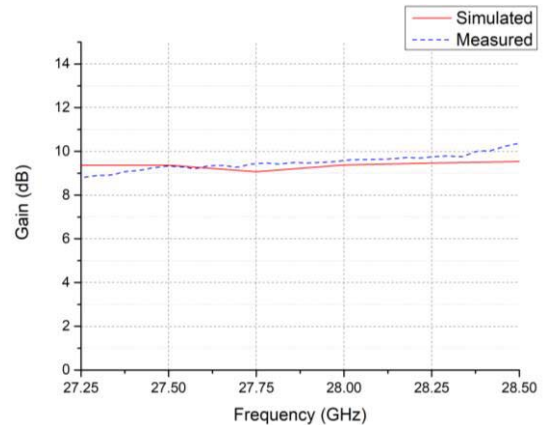
Fig. 17. Simulated and measured  $S_{11}$  comparison.

Fig. 18. Simulated and measured peak gain comparison.

The measured peak gain varies from 8.8 to 10.3 dBi from 27.25 to 28.5 GHz, as shown in Fig. 18.

As the azimuthal gain ripple increases, the peak gain will increase and result in increased directionality. It can also be seen in Fig. 19 that the measured azimuthal gain ripple is greater than the simulated value toward the higher end of the frequency band. Hence, the antenna shows a greater measured peak gain than the simulation (see Fig. 18) at higher frequencies.

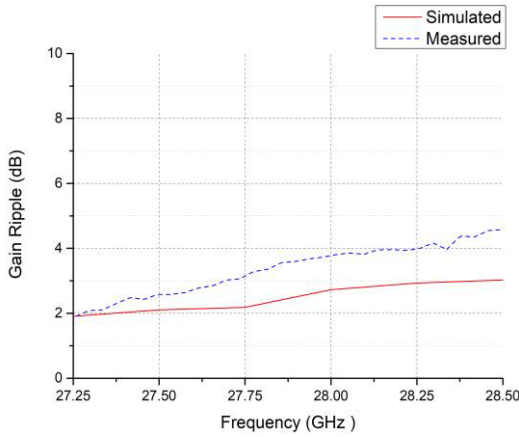


Fig. 19. Simulated and measured azimuthal gain ripple comparison.

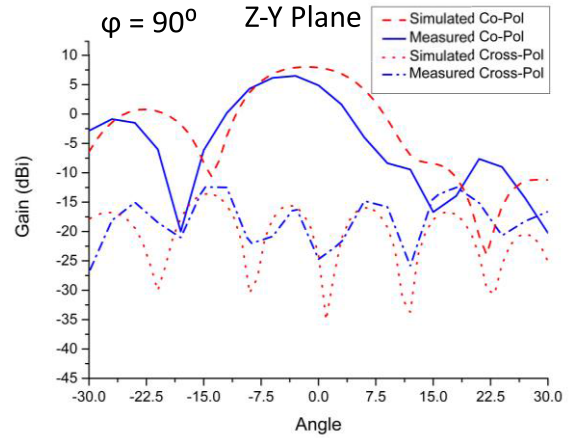


Fig. 22. Simulated and measured elevation (ZY) pattern at 28 GHz.

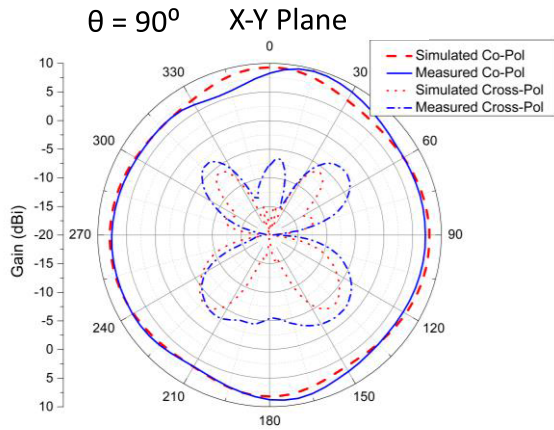


Fig. 20. Simulated and measured azimuth (XY) plane pattern at 28 GHz.

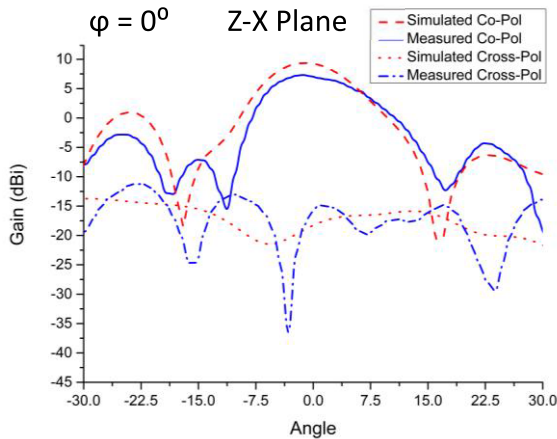


Fig. 21. Simulated and measured elevation (ZX) pattern at 28 GHz.

Fig. 19 shows that the measured azimuthal gain ripple varies from 2.10 to 4.4 dBi (27.25–28.5 GHz) over the bandwidth of 1.25 GHz (variation < 3 dB, 27.25–27.75 GHz). The azimuthal gain ripple is the smallest for the proposed design and is the most attractive in the literature to date.

TABLE II

COMPARISON WITH EXISTING MM-WAVE OMNIDIRECTIONAL ANTENNAS AND ARRAYS (\*: SIMULATED, \*\*: MEASURED)

Ref.	Freq. (GHz)	Peak Gain	Gain Ripple (max)	Length / ( $\lambda_o$ )	Configuration / Complexity
[12]**	24-29.5	11.5 dBi	>10dB	66 mm / (5.72 $\lambda_o$ )	SIW based /Complex
[13]*	25.8-29.3	12 dBi	>7dB	68mm / (6.13 $\lambda_o$ )	SIW based /Complex
[14]**	21.1-27.82	12.3 dBi	>7dB	62mm / (5.37 $\lambda_o$ )	SIW based /Complex
[15]**	34-36	10.8 dBi	<5.1dB	70mm / (8 $\lambda_o$ )	LWA feed /Complex
[16]*	27-28.5	2.08 dBic	NA	3.1mm / (0.32 $\lambda_o$ )	Coax probe /Complex
This work**	27.25-28.5	10.3 dBi	<4.4dB	67mm / (6.23 $\lambda_o$ )	MS-GCPW /Simple

Fig. 20 shows the azimuth (Z-axis) patterns at 28 GHz. Figs. 21 and 22 show the elevation patterns for the ZX and ZY planes at 28 GHz.

VI. COMPARISON WITH EXISTING MM-WAVE OMNIDIRECTIONAL ANTENNAS AND ARRAYS

There is a small number of mm-wave omnidirectional antennas reported to date. Table II compares the existing antennas with the proposed design. The reported designs [12], [13], [14] are based on SIW technology and have azimuthal gain ripple varying from 7 to 10 dB.

Zheng et al. [15] show an azimuthal gain ripple of 5.1 dB and also the peak gain variation from 4.6 to 10.8 dBi across the frequency band indicating a significant variation in the elevation pattern. In [16], the simulated design shows a gain of 2.08 dBic with a complex design and is challenging to realize an array using this element.

In comparison, the proposed design has a low profile of (6.23  $\times$  2.3  $\lambda_o$ ) while maintaining the same width as the connector region throughout the design with a peak gain of 10.3 dBi. Furthermore, it exhibits superior features, such as greater impedance bandwidth, low azimuthal gain ripple, and less peak gain variation over the frequency band.

## VII. CONCLUSION

In this design, a novel dipole with a semicircular cutout was used to develop an omnidirectional antenna array. This array design covers mm-wave bands within 27.25–28.5 GHz with best-in-class omnidirectionality. Furthermore, the compact array has a low profile, is low-cost, and is easy to fabricate, making it a viable candidate for future communications, such as mm-wave fixed wireless access points.

## REFERENCES

- [1] J. Zhang, X. Ge, Q. Li, M. Guizani, and Y. Zhang, "5G millimeter-wave antenna array: Design and challenges," *IEEE Wireless Commun.*, vol. 24, no. 2, pp. 106–112, Apr. 2017.
- [2] R. Flamini, C. Mazzucco, R. Lombardi, C. Massagrande, F. Morgia, and A. Milani, "Millimeter-wave phased arrays for 5G: An industry view on current issues and challenges," in *Proc. IEEE Int. Symp. Phased Array Syst. Technol. (PAST)*, Oct. 2019, pp. 1–2.
- [3] S. Rangan, T. S. Rappaport, and E. Erkip, "Millimeter-wave cellular wireless networks: Potential S and challenges," *Proc. IEEE*, vol. 102, no. 3, pp. 366–385, Mar. 2014.
- [4] R. Bancroft and B. Bateman, "An omnidirectional planar microstrip antenna," *IEEE Trans. Antennas Propag.*, vol. 52, no. 11, pp. 3151–3154, Nov. 2004.
- [5] L. Bras, N. B. Carvalho, and P. Pinho, "Planar omnidirectional microstrip antenna array for 5 GHz ISM and UNII band," in *Proc. IEEE Antennas Propag. Soc. Int. Symp. (APSURSI)*, Jul. 2013, pp. 1590–1591.
- [6] J. Qiu, B. Sun, L. Zhong, and W. Deng, "A novel omnidirectional high-gain microstrip antenna array," in *Proc. Asia-Pacific Microw. Conf.*, Dec. 2008, pp. 1–4.
- [7] K. Wei, J.-Y. Li, R. Xu, and G.-W. Yang, "Circularly polarized omnidirectional microstrip antenna array," in *Proc. IEEE Int. Symp. Antennas Propag. USNC/URSI Nat. Radio Sci. Meeting*, Jul. 2017, pp. 2315–2316.
- [8] H. Yi, L. Li, J. Han, and Y. Shi, "Traveling-wave series-fed patch array antenna using novel reflection-canceling elements for flexible beam," *IEEE Access*, vol. 7, pp. 111466–111476, 2019.
- [9] G. F. Hamberger, S. Trummer, U. Siart, and T. F. Eibert, "A planar dual-polarized microstrip 1-D-beamforming antenna array for the 24-GHz band," *IEEE Trans. Antennas Propag.*, vol. 65, no. 1, pp. 142–149, Jan. 2017.
- [10] H. Wang, K. E. Kedze, and I. Park, "A high-gain and wideband series-fed angled printed dipole array antenna," *IEEE Trans. Antennas Propag.*, vol. 68, no. 7, pp. 5708–5713, Jul. 2020.
- [11] R. A. Alhalabi and G. M. Rebeiz, "High-efficiency angled-dipole antennas for millimeter-wave phased array applications," *IEEE Trans. Antennas Propag.*, vol. 56, no. 10, pp. 3136–3142, Oct. 2008.
- [12] C. Mao, M. Khalily, P. Xiao, T. W. C. Brown, and S. Gao, "Planar sub-millimeter-wave array antenna with enhanced gain and reduced sidelobes for 5G broadcast applications," *IEEE Trans. Antennas Propag.*, vol. 67, no. 1, pp. 160–168, Jan. 2019.
- [13] Y. Liu, M. C. E. Yagoub, and M. Nassor, "Omni-directional antenna array with improved gain for 5G communication systems," in *Proc. IEEE USNC-CNC-URSI North Amer. Radio Sci. Meeting*, Jul. 2020, pp. 33–34.
- [14] Y. Liu and M. C. E. Yagoub, "Compact omnidirectional millimeter-wave antenna array fed in series by a novel feed network," *IEEE Trans. Antennas Propag.*, vol. 69, no. 11, pp. 7604–7612, Nov. 2021.
- [15] D. Zheng, Y.-L. Lyu, and K. Wu, "Transversely slotted SIW leaky-wave antenna featuring rapid beam-scanning for millimeter-wave applications," *IEEE Trans. Antennas Propag.*, vol. 68, no. 6, pp. 4172–4185, Jun. 2020.
- [16] W. Lin and R. W. Ziolkowski, "Compact, omni-directional, circularly-polarized mm-wave antenna for device-to-device (D2D) communications in future 5G cellular systems," in *Proc. 10th Global Symp. Millim. Waves*, May 2017, pp. 115–116.



**Neeraj Kumar Maurya** (Graduate Student Member, IEEE) received the B.Sc. degree (Hons.) in electronics from the University of Delhi, New Delhi, India, in 2011, and the M.Sc. degree in electronics with specialization in microwave and radar communication from Cochin University of Science and Technology (CUSAT), Kochi, India, in 2015. He is currently pursuing the Ph.D. degree in mm-wave antenna design from Technological University Dublin, Dublin, Ireland.

From 2015 to 2020, he was with Cambium Networks Private Ltd., Bengaluru, India, and the Antenna Company International N.V., Eindhoven, The Netherlands, as a Senior Antenna Engineer. His current research interests include sub-6 GHz and mm-wave antenna design for wireless communication.



**Max J. Ammann** (Fellow, IEEE) received the Ph.D. degree in antennas and propagation from Trinity College, University of Dublin, Dublin, Ireland, in 1997.

He is a Professor of antennas and propagation with the School of Electrical and Electronic Engineering, Technological University Dublin's, Dublin, and the Director with the Antennas and High-Frequency Research Centre. He became a Chartered Engineer in 1986. He has more than 200 peer-reviewed articles published in journals and international conferences.

His research interests include electromagnetic theory, antenna miniaturization for terminal and ultrawideband applications, antennas for medical devices, and antenna issues relating to privacy.

Dr. Ammann is a member of the IEEE International Committee for Electromagnetic Safety. His team received the 13 Best Paper Awards at International Conferences on Antennas and Propagation and seven Commercialisation Awards. He has served as an Expert to industry on various antenna technologies in the communications, medical, aviation, and electronic security sectors in Ireland and Abroad. He acted as an Associate Editor for the IEEE ANTENNAS AND WIRELESS PROPAGATION LETTERS from 2012 to 2018. He has Co-Chaired IWAT2022 in Dublin and various workshops on antennas and related technologies.



**Patrick McEvoy** (Senior Member, IEEE) received the Diploma degree in telecommunications and electronic engineering from the Dublin Institute of Technology, Dublin, Ireland, in 1995, the M.Eng. degree in electronic communications engineering from the University of Hull, Hull, U.K. (with studies at L'Institut Supérieur d'Electronique de Paris, France), in 1998, and the Ph.D. degree in microwave antenna engineering from Loughborough University, Leicestershire, U.K., in 2007.

He is a Lecturer with the School of Electrical and Electronic Engineering, Technological University Dublin's, Dublin, and a Senior Researcher with the Antennas and High-Frequency Research Centre. He has 24 years of applied academic research and industrial experience, including design, high-volume manufacturing, and measurement systems for miniaturized microwave antennas. He has authored more than 95 scientific articles and has helped organize five international conferences on antennas and propagation. His research interests include electromagnetic theory, antenna miniaturization handheld, and medical and energy harvesting applications.

Dr. McEvoy was a Co-Recipient of two awards for Industrial Commercialization of Researched Antenna Technologies and the 2014 Computer Simulation Technology University Publication Award.